Biophysical Chemistry, 45 (1993) 253–272
Elsevier Science Publishers B.V., Amsterdam

BIOCHE 01717

Pump and exchanger mechanisms in a model of smooth muscle

F.K. Skinner, C.A. Ward and B.L. Bardakjian

Institute of Biomedical Engineering and Department of Mechanical Engineering, University of Toronto, Toronto, Ont. (Canada)

(Received 2 December 1991; accepted in revised form 28 August 1992)

Abstract

A novel approach to modelling pump and exchanger mechanisms is presented. In this approach, new thermodynamic expressions for the calcium pump, sodium–calcium exchanger and sodium–potassium pump are developed using statistical rate theory (SRT). This theory is well-defined and is not derived empirically. This is in contrast to previous thermodynamic pump expressions which used a simple linear relationship or relied on empirical data for their functional form. The functional form of these new expressions does not require assumptions of steady state or particular forms of voltage dependencies in specific steps. Also, the explicit reaction scheme is not required. Instead, assumptions of a rate-limiting step in the scheme and a near-equilibrium ratio of intermediate substrates are required. These expressions are incorporated into an overall model of gastric smooth muscle. This model presents a novel approach whereby thermodynamic representations for calcium pumps, sodium–calcium exchangers and sodium–potassium pumps have been included together in a model of ionic transport mechanisms for smooth muscle. Variations in basal metabolic concentrations are used to explain the observed amplitude variation in the transmembrane voltage of gastric smooth muscle. The interaction of the various mechanisms are used to illustrate the large depolarization obtained in smooth muscle with ouabain as well as the forward and reverse modes of the sodium–calcium exchanger.

Keywords: Calcium pump; Sodium–calcium exchanger; Sodium–potassium pump; Nonequilibrium thermodynamics; Statistical rate theory; Gastric smooth muscle

1. Introduction

Ionic transport across excitable cell membranes occurs via channels, pumps and exchangers. Channels are voltage and/or ligand gated and movement occurs due to concentration and potential gradients. Pumps require energy and work against the concentration gradient. The presence of pumps in the cell membrane is essential for the proper functioning of the cell. They allow an asymmetric distribution of ionic concentrations to be maintained which in turn is necessary for the generation of voltage oscillations. In this paper, we use a nonequilibrium thermodynamic approach, statistical rate theory (SRT) [1], to develop expressions for the calcium pump, the sodium–calcium exchanger and the sodium–potassium pump. These active transport mecha-

Correspondence to: Frances K. Skinner, Department of Chemistry, Brandeis University, Waltham, MA 02254-9110 (USA)

nisms are then included in a model of the transmembrane voltage in gastric smooth muscle. The oscillatory nature of gastric smooth muscle as well as the various ionic channels also form part of the model.

There has not been extensive work done on the theoretical modelling of pumps and exchangers partly due to the difficulty in obtaining experimental data. This is in contrast to channels where modelling has been performed on molecular, single channel and whole cell levels. The modelling of pumps and exchangers that has been done can be divided into essentially three major groups: First, there are the simple models for pumps which are diffusional in nature in that they extend the Goldman–Hodgkin–Katz (GHK) voltage equation by incorporating active transport systems in addition to the passive permeabilities that are already there (e.g. [2,3]). Second, and the most common, there are models which use explicit kinetic schemes which are analyzed in some detail, using forward and backward rates for each step (e.g., [4,5]). Third, there are models that rely on nonequilibrium thermodynamics to analyze the fluxes (e.g., [6,7]).

Calcium pumps, sodium–calcium exchangers and sodium–potassium pumps are not usually considered together in models of excitable cells. Overall ionic transport models have either focused on a particular active transport mechanism such as an explicit sodium–potassium kinetic scheme in a model of cardiac cells [8], or used simple relationships such as a linear dependence on the intracellular calcium for the calcium pump [9] or a one-way channel [10]. In cardiac cells, the contribution of both sodium–potassium pumps and sodium–calcium exchangers have been considered [11,12]. Pumps and exchangers work together to maintain low intracellular concentrations of sodium and particularly calcium [13]. It is not possible to isolate their behaviour from the rest of the cell. A model is a convenient way to study the entire cellular system with its many interactions. For the model in this paper of the transmembrane voltage in gastric smooth muscle, it is not possible to consider only the sodium–potassium pump or the calcium pump or the sodium–calcium exchanger. The calcium pump and the sodium–calcium exchanger [14,15] are needed to maintain the low intracellular calcium concentration, and the sodium–potassium pump [16] removes sodium and brings in potassium to maintain their respective gradients. They must all be dealt with in the model. In addition, evidence of metabolic regulation of the electrical activity in smooth muscle [17] increases the importance of including pump mechanisms in some detail.

The expressions which we develop for the calcium pump, sodium–calcium exchanger and sodium–potassium pump use a common approach: nonequilibrium thermodynamics described in terms of SRT. In application to rates of processes, SRT has led to an improved expression for the rate of a broad range of processes, including chemical reactions [18], absorption at a liquid–gas interface [19], and absorption at a gas–solid interface [20]. The improved expressions generally give a higher rate in the period immediately after the process is initiated. The predictions in each case have been found to compare favourably with experimental data. Since pump and exchanger mechanisms are represented as a series of chemical reactions or schemes, SRT can be used to determine their rates.

We report the effects of the pumps and exchangers in the model, as determined by a parametric study of the membrane voltage in gastric smooth muscle. The interaction or coupling of the various mechanisms is theoretically based on the electrochemical potential. This is in contrast to the interaction between several kinetic schemes where the coupling would depend on the particular step(s) chosen to be voltage dependent as well as the form of the voltage dependence. The aims of this paper are to develop new thermodynamic expressions for pumps and exchangers and to use these expressions in an overall model of gastric smooth muscle. We are handicapped by the lack of experimental data that can be used to evaluate the approach, but we note that the basis of our approach, SRT, has been examined for physical systems [18–20] for a range of processes. In each case, experimental support has been found. Thus we propose to determine what results can be obtained for a biological system using a theory

that works for nonequilibrium physical systems. This approach is considered as an alternative to that of explicit kinetic schemes. To simplify the presentation of the whole cell model, the passive transport mechanism have not been presented in detail here, but are discussed elsewhere [21]. The form of the equation used is shown in the appendix to the present paper.

2. Gastric smooth muscle

2.1 Description

Muscular contractions in the mammalian stomach are governed by myogenic, neural and hormonal control systems. The myogenic control system causes the smooth muscle cells to produce periodic depolarizations or autonomous electrical oscillations which are known as the electrical control activity (ECA) or slow waves. The slow wave plays an important role in controlling the motility of the distal stomach and the intestines. It 'primes' the cells for contraction (pacemaker oscillations) in that the slow wave can trigger repetitive spike activity on top of the depolarization, the strength of the contraction being related to the frequency of the spike bursts [22].

The stomach can be divided into three regions: the fundus, the corpus and the antrum. In the fundus there are no electrical oscillations but there is an underlying resting membrane voltage. The corpus and the antrum both exhibit autonomous electrical oscillations [23]. When electrical activity from detached pieces of muscle is observed, the ECA in gastric smooth muscle from different regions of the stomach, varies in frequency, waveshape and magnitude. Szurszewski [23] points out two oppositely oriented gradients in the intrinsic magnitude of the membrane voltage: in the aborad direction, the resting membrane voltage decreases, but the voltage amplitude and the maximum rate of rise of the upstroke increases.

Spontaneous rhythmic contractions of gastrointestinal smooth muscle have been observed for a long time leading to questions such as where the site of generation of these oscillations is located and how and why these oscillations occur. The identification of the site of generation is controversial and is not helped by the structural complexity of smooth muscle, with extensive networks of neurons and of interstitial cells of Cajal. An inner layer of circular muscle is surrounded by an outer longitudinal muscle layer. The individual cells in each layer are connected to each other via low resistance gap junctions which allow current to spread through the various layers.

The oscillatory behaviour in smooth muscle is believed to be due to cytoplasmic or metabolic clock (for example, an oscillation in cyclic AMP and calcium) [24]. In a review, Connor [25] showed that the mechanisms which generate the electrical oscillations are quite closely coupled to metabolic processes. It was also found that ouabain depolarized the membrane by an amount which could exceed the slow wave amplitude. Experimental evidence suggests that these oscillations are not generated by membrane voltage changes. In the guinea pig stomach [22,26], the slow wave was found to be generated by a voltage independent process which was believed to be metabolic. More recently, in canine colon smooth muscle [17], it was shown that a voltage change was not responsible for the generation of the upstroke potential of the slow wave. Slow waves were also found to be sensitive to metabolic inhibition [27]. Most importantly, slow waves are not preceded by a prepotential or gradual depolarization, typical of membrane oscillators [22,25]. The slow wave rises abruptly from a steady resting membrane voltage. When smooth muscle is voltage clamped it produces spontaneous inward currents whose frequencies are identical to the free-running voltage oscillation. In most other membrane oscillators voltage clamping eliminates the rhythmical fluctuations in membrane current [25,28,29].

2.2 Active transport mechanisms

The observed behaviour of smooth muscle has led to the development of a model in which the oscillatory behaviour is not generated by an interplay of different channel types, but by an inde-

pendent clock mechanism [10,30]. The importance of active transport mechanisms (due to their metabolic control) in smooth muscle suggests that these mechanisms should not be excluded in any overall model of transmembrane voltage in smooth muscle. The energy which drives the pump mechanisms is derived from the splitting of adenosine triphosphate (ATP), a metabolic component whose concentration is not static. Therefore, we introduce the pump transmission coefficient to represent the oscillatory and normalized time-variation of metabolic components. At each instant in time, the metabolic concentrations are determined by the pump transmission coefficient (normalized value) times the particular concentrations. An alternative is to use rate equations for the changing metabolic concentrations [31]. However, no specific data for smooth muscle is available for this option.

The active transport mechanisms in the overall model are used to address four issues: (i) the effect of ouabain on the transmembrane voltage, (ii) the forward and reverse modes of the sodium-calcium exchanger, (iii) the observed gradient in the intrinsic magnitude of the transmembrane voltage, and (iv) prepotentials.

3. Theory

3.1 Statistical rate theory

The basic assumption of SRT is that single molecular events result in the transport of molecules from one phase to another [1]. The quantum mechanical transition probability is used to predict the probability of a transition from one molecular distribution to another at a particular instant in time. This probability is expressed in terms of the appropriate number of microscopic states. According to the Boltzmann definition of entropy, the number of states available to a system is related to the entropy of the system:

$$S(\lambda_s) = k \ln \Omega(\lambda_s) \tag{1}$$

where S is the entropy, λ_s is a molecular distribution, k is Boltzmann's constant and Ω is the number of microscopic states corresponding to the molecular distribution λ_s. For a macroscopic system, the rate at which the system would make a transition from molecular distribution λ_i to molecular distribution λ_j, $j(\lambda_i, \lambda_j)$, is given by:

$$j(\lambda_i, \lambda_j) = K(\lambda_i, \lambda_j) \exp\left(\frac{S(\lambda_j) - S(\lambda_i)}{k}\right) \tag{2}$$

where $K(\lambda_i, \lambda_j)$ is the average rate of transfer from a microscopic state of λ_i to a microscopic state of λ_j. The net rate of molecular transport from volume ξ to volume ζ is:

$$j_{\xi\zeta} = K(\lambda_i, \lambda_j) \exp\left(\frac{S(\lambda_j) - S(\lambda_i)}{k}\right) - K(\lambda_i, \lambda_h) \exp\left(\frac{S(\lambda_h) - S(\lambda_i)}{k}\right). \tag{3}$$

The local equilibrium assumption is used within each phase to evaluate the entropy difference; the thermodynamic state of each of the small volumes (within volume ξ or ζ) can be described in terms of the local equilibrium variables of that small volume. However, equilibrium does not exist between the two volumes ξ and ζ. The entropy of the system is taken to be the sum of the entropies of each of the small volumes. The Euler relation expresses the entropy in terms of the other thermodynamic properties.

The temperature is assumed to be the same in volumes ξ and ζ with the individual volumes being constant. Energy transport of a single component is assumed to occur only between volumes ξ and ζ, since it is only between these two volumes that exchange is taking place when the molecular distribution goes from λ_i to λ_j. The net rate of molecular transfer from volume ξ to volume ζ becomes [1]:

$$j_{\xi\zeta}(\lambda_i) = K(\lambda_i, \lambda_j)\delta_{\xi\zeta} - K(\lambda_i, \lambda_h)\delta_{\xi\zeta}^{-1} \tag{4}$$

where

$$\delta_{\xi\zeta}(\lambda_i) = \exp\left(\frac{\mu_\gamma^\xi(\lambda_i) - \mu_\gamma^\zeta(\lambda_i)}{kT}\right), \tag{5}$$

μ_γ^ξ, μ_γ^ζ are the chemical potentials of species γ in volume ξ or volume ζ and T is the temperature.

Finally, it is assumed that the average rate of transport between microscopic states of neighboring molecular distributions is the same for all molecular distributions near global equilibrium. This yields:

$$j_{\xi\zeta}(\lambda_i) = K_{\xi\zeta}(\lambda_{\text{equil}})\left[\delta_{\xi\zeta}(\lambda_i) - \delta_{\xi\zeta}^{-1}(\lambda_i)\right] \qquad (6)$$

where $j_{\xi\zeta}(\lambda_i)$ is the instantaneous molecular rate of transport between the volumes and $K_{\xi\zeta}(\lambda_{\text{equil}})$ is the equilibrium exchange rate between volumes. The use of this equilibrium exchange rate does not imply that the rate of transfer is also at equilibrium. This assumption has been the subject of a number of different experimental investigations [1,18–20,32]. The nonequilibrium aspect of eq. (6) is due to the 'δ' part of the equation. Nonequilibrium results from a different number of microscopic states, Ω, in the different molecular distributions.

3.2 Application of SRT to pump and exchanger modelling

If a particular step in the pump or exchanger scheme is assumed to be rate-limiting, then the net rate of the reaction, j, (as determined by the rate-limiting step) is given by eq. (6):

$$j = K(\delta - \delta^{-1}) \qquad (7)$$

where K is the equilibrium exchange rate for the particular step and

$$\delta = \exp\left(\frac{\sum_l \mu_l - \sum_r \mu_r}{RT}\right), \qquad (8)$$

$\sum_l \mu_l$ is the sum of the electrochemical potentials on the left side of the reaction and $\sum_r \mu_r$ is the sum of the electrochemical potentials on the right side of the reaction [18]. For example for the reaction:

$$A + B \rightleftharpoons C + D, \qquad (9)$$

$$\sum_l \mu_l = \mu_A + \mu_B \qquad (10)$$

$$\sum_r \mu_r = \mu_C + \mu_D. \qquad (11)$$

The electrochemical potential of component B is:

$$\mu_B = \mu_B^0(T, P, \nu) + RT \ln a_B + zF\phi \qquad (12)$$

where μ^0 is the reference chemical potential dependent on temperature (T), pressure (P) and solubility (ν), a is the activity, R is the gas constant, z is the valency, F is Faraday's constant and ϕ is the electrical potential. The other components (A, C, D) would have a similar form.

The development of specific expressions for the calcium pump, the sodium–potassium pump and the sodium–calcium exchanger is now described. The calcium pump is developed first since it involves only one ionic species. Next, the sodium–calcium exchanger and then the sodium–potassium pump, where most of the previous modelling has been done.

3.2.1 The calcium pump

Calcium plays a major role in the contraction of smooth muscle. The intracellular calcium is about four orders of magnitude less than extracellular calcium. Calcium pumps are known to exist in smooth muscle [33,34] and contribute to the maintenance of this low intracellular calcium concentration.

Proposed reaction schemes or enzyme cycles are present in the literature [13,35,36] and there is a one-to-one stoichiometry of calcium to ATP [13,36]. The reaction cycle (for erythrocyte enzyme) is given by the following set of equations:

$$ATP + E_1 + Ca_i \rightleftharpoons CaE_1 \sim P + ADP \qquad (13)$$

$$CaE_1 \sim P \rightleftharpoons CaE_2 \sim P \qquad (14)$$

$$CaE_2 \sim P \rightleftharpoons Ca_e + E_2 + P_i \qquad (15)$$

$$E_2 \rightleftharpoons E_1 \qquad (16)$$

where ATP, ADP, P_i are adenosine triphosphate, adenosine diphosphate and inorganic phosphate respectively, Ca_i, Ca_e are intracellular and extracellular calcium, respectively, and E_1, E_2 are two different conformational enzyme states. The calcium ATPase found in smooth muscle is similar to erythrocyte calcium ATPase [34] so that the enzyme reaction cycle most likely applies to smooth muscle also. The enzyme exists in two

different states E_1 and E_2 corresponding to two different conformations on opposite sides of the membrane. The formation of $CaE_1 \sim P$ is endergonic but the reaction would be pulled in the direction of formation of E_2 and P_i by the strongly exergonic character of step (15), which would drive the entire reaction cycle [35].

If the overall reaction scheme is at equilibrium, it can be reduced to the single reaction:

$$ATP + Ca_i = ADP + P_i + Ca_e \tag{17}$$

which thermodynamically implies:

$$\mu_{ATP} + \mu_{Ca_i} = \mu_{ADP} + \mu_{P_i} + \mu_{Ca_i}, \tag{18}$$

The electrochemical potentials are defined as:

$$\mu_{ATP} = \mu^0_{ATP}(T, P, \nu) + RT \ln a_{ATP} \tag{19}$$

$$\mu_{ADP} = \mu^0_{ADP}(T, P, \nu) + RT \ln a_{ADP} \tag{20}$$

$$\mu_{P_i} = \mu^0_{P_i}(T, P, \nu) + RT \ln a_{P_i} \tag{21}$$

$$\mu_{Ca_i} = \mu^0_{Ca_i}(T, P, \nu) + RT \ln a_{Ca_i} + 2F\phi^i \tag{22}$$

$$\mu_{Ca_e} = \mu^0_{Ca_e}(T, P, \nu) + RT \ln a_{Ca_e} + 2F\phi^e \tag{23}$$

where μ^0 is the reference electrochemical potential dependent on temperature (T), pressure (P) and solubility (ν), a is the activity and ϕ is the electrical potential, F is Faraday's constant and R is the gas constant. The equilibrium voltage for the calcium pump is given by:

$$V_{Ca,p} = \frac{RT}{2F}\left\{\ln\left(\frac{[ADP][P_i][Ca]_e}{[ATP][Ca]_i}\right) + \frac{\left(\mu^0_{Ca_e} - \mu^0_{Ca_i}\right) + \left(\mu^0_{ADP} + \mu^0_{P_i} - \mu^0_{ATP}\right)}{RT}\right\} \tag{24}$$

where $V_{Ca,p} = (\phi^i - \phi^e)_{equil}$ is the equilibrium voltage for the calcium pump or the voltage at which the calcium pump current density changes direction. The activities and the concentrations are assumed to be the same.

Statistical rate theory is used to obtain an expression for the rate of a particular step, such as step (13), which is chosen as the rate-limiting step. The net rate of reaction (13), j is given by eq. (7), where K is the equilibrium exchange rate of the reaction (13), and

$$\delta = \left(\frac{[ATP][E_1][Ca]_i}{[CaE_1 \sim P][ADP]}\right) \times \exp\left\{\frac{\mu^0_{ATP} + \mu^0_{E_1} + \mu^0_{Ca_i} - \mu^0_{CaE_1 \sim P} - \mu^0_{ADP} + 2F\phi^i}{RT}\right\}. \tag{25}$$

The rest of the steps in the reaction scheme are approximated to be near equilibrium with respect to the rate-limiting step. They can be reduced to:

$$Ca_{E_1 \sim P} = Ca_e + P_i + E_1 \tag{26}$$

which implies:

$$\mu_{Ca_{E_1 \sim P}} = \mu_{Ca_e} + \mu_{P_i} + \mu_{E_1} \tag{27}$$

and

$$\mu^0_{CaE_1 \sim P} - \mu^0_{Ca_e} - \mu^0_{P_i} - \mu^0_{E_1} - 2F\phi^e = RT \ln\left(\frac{[Ca]_e[P_i][E_1]}{[CaE_1 \sim P]}\right). \tag{28}$$

In eq. (25), if we assume that

$$\left(\frac{[E_1]}{[CaE_1 \sim P]}\right) \approx \left(\frac{[E_1]}{[CaE_1 \sim P]}\right)_{equil}, \tag{29}$$

then eq. (28) (an approximate equilibrium situation), can be substituted into eq. (25) to obtain an approximation to δ, say δ':

$$\delta' = \left(\frac{[ATP]}{[ADP][P_i]}\right)\left(\frac{[Ca]_i}{[Ca]_e}\right) \times \exp\left\{\left[\left(\mu^0_{ATP} - \mu^0_{ADP} - \mu^0_{P_i}\right) + \left(\mu^0_{Ca_i} - \mu^0_{Ca_e}\right) + 2FV_m\right]/RT\right\} \tag{30}$$

where $V_m = \phi^i - \phi^e$ is the transmembrane voltage. Thus, the rate of the overall reaction, $j_{Ca,p}$, as determined by the chosen rate-limiting step, is given by:

$$j_{Ca,p} = K_{Ca,p}\left(\delta_{Ca,p} - \delta^{-1}_{Ca,p}\right) \tag{31}$$

where

$$\delta_{Ca,p} = \kappa_{pump}\left(\frac{[ATP]}{[ADP][P_i]}\right)\left(\frac{[Ca]_i}{[Ca]_e}\right) \times \exp\left\{\left[\left(\mu^0_{ATP} - \mu^0_{ADP} - \mu^0_{P_i}\right) + \left(\mu^0_{Ca_i} - \mu^0_{Ca_e}\right) + 2FV_m\right]/RT\right\} \quad (32)$$

and $K_{Ca,p}$ is the equilibrium exchange rate for the reaction (13), and κ_{pump} is the pump transmission coefficient or the oscillatory and normalized time-variation of metabolic components discussed above. This time-variation κ_{pump}, could refer to [ATP], [ADP] and $[P_i]$ or to some combination of them such as the ratio of [ATP] to [ADP]. Since the reaction cycle results in the extrusion of one calcium ion, the calcium pump current density $J_{Ca,p}$, is:

$$J_{Ca,p} = 2FK_{Ca,p}\left(\delta_{Ca,p} - \delta^{-1}_{Ca,p}\right) \quad (33)$$

where outward current density is positive. As mentioned earlier, the nonequilibrium is due to the "δ" part of the eq. (31) and in eq. (32) can be seen to be due to concentration and voltage changes and intracellular and extracellular solubility differences.

Equation (31) was obtained by choosing step (13) as the rate-limiting step. If we chose step (15) (or any other step in the scheme) as the rate-limiting step, we would have obtained the same functional form as eq. (31) except that $K_{Ca,p}$ would be the equilibrium exchange rate for step (15) and the required assumption would be:

$$\left(\frac{[CaE_2 \sim P]}{[E_2]}\right) \approx \left(\frac{[CaE_2 \sim P]}{[E_2]}\right)_{equil}. \quad (34)$$

In other words, the functional form of eq. (31) does not depend on the choice of the rate-limiting step.

3.2.2 *The sodium–calcium exchanger*

The sodium–calcium exchanger is another mechanism which is responsible for controlling intracellular calcium. Its stoichiometry is found to be 3:1 for Na:Ca and ATP is not considered to play a direct role [37,38]. There is experimental evidence for the presence of a sodium–calcium exchanger in smooth muscle [39,40].

For the exchanger there is a general scheme of Stein [41] which was developed for antiporters or exchange-only carriers. Johnson and Kootsey [41] proposed a minimum mechanism for the sodium–calcium exchanger whose behaviour qualitatively agreed with experimental data. Overall, the reaction is:

$$3Na_e + Ca_i \rightleftharpoons 3Na_i + Ca_e \quad (35)$$

where Na_i, Na_e are intracellular and extracellular sodium, respectively. Equilibrium of the equation implies:

$$3\mu_{Na_e} + \mu_{Ca_i} = 3\mu_{Na_i} + \mu_{Ca_e} \quad (36)$$

where

$$\mu_{Na_i} = \mu^0_{Na_i}(T, P, \nu) + RT \ln a_{Na_i} + F\phi^i \quad (37)$$

$$\mu_{Na_e} = \mu^0_{Na_e}(T, P, \nu) + RT \ln a_{Na_e} + F\phi^e. \quad (38)$$

The equilibrium voltage for the sodium–calcium exchanger is:

$$V_{NaCa,e} = \frac{RT}{F}\left\{\ln\left(\left(\frac{[Na]_i}{[Na]_e}\right)^3\left(\frac{[Ca]_e}{[Ca]_i}\right)\right) + \frac{3\left(\mu^0_{Na_i} - \mu^0_{Na_e}\right) + \left(\mu^0_{Ca_e} - \mu^0_{Ca_i}\right)}{RT}\right\} \quad (39)$$

where $V_{NaCa,e} = (\phi^i - \phi^e)_{equil}$ is the equilibrium voltage for the sodium–calcium exchanger or the voltage at which the current density of the exchanger changes direction. The activities and concentrations are assumed to be the same. At equilibrium, if there is no difference between the sodium and calcium extracellular and intracellular reference potentials, that is, the temperature, pressure and solubilities are the same, then:

$$\left(\frac{[Na]_i}{[Na]_e}\right)^3\left(\frac{[Ca]_e}{[Ca]_i}\right) = \exp\left(\frac{FV_{NaCa,e}}{RT}\right). \quad (40)$$

This relationship is commonly found in the literature (e.g. [13]) for the more general situation of a

n:1 stoichiometry for the sodium–calcium exchanger, i.e.,

$$\left(\frac{[Na]_e}{[Na]_i}\right)^n\left(\frac{[Ca]_i}{[Ca]_e}\right)=\exp\left\{(2-n)\left(\frac{FV_{NaCa,e}}{RT}\right)\right\}. \tag{41}$$

In the absence of specific experimental data for smooth muscle, a rate-limiting step in the mechanism is assumed. In this way, the same procedure as used for the calcium pump could be used to obtain an expression for the sodium–calcium exchanger current density. The procedure is the following: (i) A step in the scheme is chosen to be rate-limiting so that the rest of the reaction scheme is near equilibrium with respect to the rate-limiting step, (ii) some ratio of intermediates, such as substrates adsorbed onto the enzyme, is assumed to be approximately equal to its equilibrium value, (iii) SRT then gives the net rate of the rate-limiting reaction, which is the rate of the overall reaction scheme. For the sodium–calcium exchanger, the rate of the overall reaction, $j_{NaCa,e}$, is:

$$j_{NaCa,e}=K_{NaCa,e}\left(\delta_{NaCa,e}-\delta_{NaCa,e}^{-1}\right) \tag{42}$$

where

$$\delta_{NaCa,e}=\left(\frac{[Na]_e}{[Na]_i}\right)^3\left(\frac{[Ca]_i}{[Ca]_e}\right)\times\exp\left\{\frac{3\left(\mu^0_{Na_e}-\mu^0_{Na_i}\right)+\left(\mu^0_{Ca_i}-\mu^0_{Ca_e}\right)-FV_m}{RT}\right\} \tag{43}$$

and $K_{NaCa,e}$ is the equilibrium exchange rate for the rate-limiting step in the reaction scheme. In this case, the reaction cycle results in the extrusion of one calcium ion and the intrusion of three sodium ions. Thus, the current density of the sodium–calcium exchanger, $J_{NaCa,e}$, is:

$$J_{NaCa,e}=-FK_{NaCa,e}\left(\delta_{NaCa,e}-\delta_{NaCa,e}^{-1}\right). \tag{44}$$

3.2.3 The sodium–potassium pump

Finally, we consider the sodium–potassium pump where most of the modelling work has been done. More detail is known about a reaction scheme for the sodium-potassium pump than either the calcium pump or the sodium–calcium exchanger. For example, there is the Albers–Post model used by Läuger and Apell [43] and the Guidotti scheme used by Chapman et al. [5]. A major consideration in kinetic analyses is determining the voltage dependences of the forward and backward rates in each step of the particular scheme. Thermodynamic approaches require explicit expressions for the unidirectional reaction rates to determine the flux induced by the sodium–potassium pump. Chapman et al. [6] used a formulation which was based on experimental observations, and Rapoport [7] used a nonequilibrium thermodynamic approach which assumed that the pumping rate depended linearly on how far the reaction was removed from equilibrium. DeWeer [44] has found this assumption to be unsatisfactory since "enzyme reactions are, in general, not driven at rates proportional to their driving force, especially when far from equilibrium".

This assumption is not required with SRT. The latter theory was derived using quantum and statistical mechanics, and the functional form of the rate expressions are neither determined empirically nor assumed to depend linearly on how far the reaction is removed from equilibrium. For the sodium–potassium pump, we consider the reaction cycle of Guidotti, taken from Chapman et al. [5]:

$$E\cdot ATP+3Na_i \rightleftharpoons Na_3E\cdot ATP \tag{45}$$

$$Na_3E\cdot ATP \rightleftharpoons Na_3E\cdot P+ADP \tag{46}$$

$$Na_3E\cdot P \rightleftharpoons E'P+3Na_e \tag{47}$$

$$E'P+2K_e \rightleftharpoons K_2E'+P_i \tag{48}$$

$$K_2E'+ATP \rightleftharpoons K_2E\cdot ATP \tag{49}$$

$$K_2E\cdot ATP \rightleftharpoons E\cdot ATP+2K_i \tag{50}$$

where K_i, K_e are intracellular and extracellular potassium respectively and E, E′ refer to conformationally distinct forms of the enzyme. The overall reaction is:

$$ATP+3Na_i+2K_e \rightleftharpoons ADP+P_i+3Na_e+2K_i. \tag{51}$$

Equilibrium of the equation implies:

$$\mu_{ATP} + 3\mu_{Na_i} + 2\mu_{K_e} = \mu_{ADP} + \mu_{P_i} + 3\mu_{Na_e} + 2\mu_{K_i} \quad (52)$$

where

$$\mu_{K_i} = \mu^0_{K_i}(T, P, \nu) + RT \ln a_{K_i} + F\phi^i \quad (53)$$

$$\mu_{K_e} = \mu^0_{K_e}(T, P, \nu) + RT \ln a_{K_e} + F\phi^e \quad (54)$$

which gives the equilibrium voltage for the sodium–potassium pump:

$$V_{NaK,p} = \frac{RT}{F}\left\{\ln\left(\left(\frac{[Na]_e}{[Na]_i}\right)^3\left(\frac{[K]_i}{[K]_e}\right)^2\left(\frac{[ADP][P_i]}{[ATP]}\right)\right) + \left[3\left(\mu^0_{Na_e} - \mu^0_{Na_i}\right) + 2\left(\mu^0_{K_i} - \mu^0_{K_e}\right) + \left(\mu^0_{ADP} + \mu^0_{P_i} - \mu^0_{ATP}\right)\right]/RT\right\} \quad (55)$$

where $V_{NaK,p} = (\phi^i - \phi^e)_{equil}$ is the equilibrium voltage of the sodium–potassium pump or the voltage at which the sodium–potassium pump current density changes direction. The activities and concentrations are assumed to be the same.

The rate-limiting step in Guidotti's scheme is chosen as the extrusion of sodium, step (47), since this is considered to be the slowest step [5]. The rate of the overall reaction, $j_{NaK,p}$, as determined by the rate-limiting step is:

$$j_{NaK,p} = K_{NaK,p}\left(\delta_{NaK,p} - \delta^{-1}_{NaK,p}\right) \quad (56)$$

where

$$\delta_{NaK,p} = \kappa_{pump}\left(\frac{[ATP]}{[ADP][P_i]}\right)\left(\frac{[Na]_i}{[Na]_e}\right)^3\left(\frac{[K]_e}{[K]_i}\right)^2 \times \exp\left\{\left[\left(\mu^0_{ATP} - \mu^0_{ADP} - \mu^0_{P_i}\right) + 3\left(\mu^0_{Na_i} - \mu^0_{Na_e}\right) + 2\left(\mu^0_{K_e} - \mu^0_{K_i}\right) + FV_m\right]/RT\right\} \quad (57)$$

and $K_{NaK,p}$ is the equilibrium exchange rate for the reaction with:

$$\left(\frac{[Na_3E \cdot P]}{[E'P]}\right) \approx \left(\frac{[Na_3E \cdot P]}{[E'P]}\right)_{equil} \quad (58)$$

Similar to the calcium pump formulation, we include the pump transmission coefficient, κ_{pump}, which represents the oscillatory and normalized time-variation of metabolic components. The reaction cycle results in the extrusion of three sodium ions and the intrusion of two potassium ions. The current density of the sodium–potassium pump, $J_{NaK,p}$, is:

$$J_{NaK,p} = FK_{NaK,p}\left(\delta_{NaK,p} - \delta^{-1}_{NaK,p}\right). \quad (59)$$

Again, as described for the calcium pump, different choices for the rate-limiting step would not change the functional form of the expression.

The procedure used to obtain the pump and exchanger expressions assumed a rate-limiting step in the reaction scheme. However, the functional form of the obtained expression is independent of the particular rate-limiting step. This implies that if different physiological conditions resulted in different rate-limiting steps, the expressions obtained would not change. What does change is the ratio of intermediates that is assumed to be close to equilibrium and the equilibrium exchange rate value, K.

4. Whole cell model

To determine how the pumps and exchangers contribute to the cell membrane voltage, an overall model of gastric smooth muscle is developed. In this model, the ionic channels are described by a generalized GHK current equation [21]. This generalization allows nonequilibrium to exist at the bulk/channel interfaces. The oscillatory nature of the electrical control activity in gastric smooth muscle forms an integral part of the model. The oscillations in the model are *not* generated by membrane events such as an interplay of two separate channels (which lead to

alternating phases of depolarization and hyperpolarization in the voltage waveform). The oscillations are metabolic, and the ATP concentration or some combination of metabolic components (which are parameters in the pump expressions) are assumed to oscillate. The subcellular or metabolic clock is modelled by two nonlinear differential equations [30] which directly affect the pump and channel mechanisms via transmission coefficients. For the channels, the transmission coefficient represents the fraction of open channels in the cell. For the pumps, the transmission coefficient represents a normalized variation in the metabolic concentrations.

The gastric smooth muscle model incorporates the following mechanisms: (i) voltage-dependent calcium channels, (ii) voltage-dependent potassium channels, (iii) calcium-dependent potassium channels, (iv) voltage-dependent sodium channels, (v) calcium pumps, (vi) sodium–potassium pumps, and (vii) sodium–calcium exchangers. The inclusion of the new thermodynamic expressions for the active transport mechanisms allow dynamic interactions to occur between the calcium pump, the sodium–calcium exchanger and the sodium–potassium pump via the voltage, intracellular and extracellular concentrations, metabolic components and the energy available from ATP splitting. These interactions arise naturally from the electrochemical potential. This is in contrast to interactions between several kinetic schemes, say, where the coupling would depend on the particular step(s) chosen to be voltage dependent and the form of the voltage dependence. The pump or exchanger's behaviour alone is difficult to study experimentally because of a lack of specific inhibitors and its interaction with other ionic transport mechanisms.

The model is given by the following equations:

$$C_m \frac{dV_m}{dt} = -J_{ionic} \tag{60}$$

$$J_{ionic} = J_K + J_{K(Ca)} + J_{Ca} + J_{Na} + J_{NaK,p} + J_{Ca,p} + J_{NaCa,e} \tag{61}$$

where C_m is the specific membrane capacitance, V_m is the membrane voltage, t is time, J_{ionic} is the total ionic current density, and J_K, $J_{K(Ca)}$, J_{Ca}, J_{Na}, $J_{NaK,p}$, $J_{Ca,p}$, $J_{NaCa,e}$ are the potassium, calcium-dependent potassium, calcium, sodium, sodium–potassium pump, calcium pump and sodium–calcium exchanger current densities, respectively. The expressions for the channel current densities are given by a generalized form of the GHK current equation and their form is shown in Appendix A.

The intracellular concentrations change according to:

$$\frac{d[K]_i}{dt} = \frac{1}{F\rho}\left(-J_K - J_{K(Ca)} + 2J_{NaK,p}\right) \tag{62}$$

$$\frac{d[Ca]_i}{dt} = \frac{f}{2F\rho}\left(-J_{Ca} - J_{Ca,p} + 2J_{NaCa,e}\right) \tag{63}$$

$$\frac{d[Na]_i}{dt} = \frac{1}{F\rho}\left(-J_{Na} - 3J_{NaK,p} - 3J_{NaCa,e}\right) \tag{64}$$

where $[K]_i$, $[Ca]_i$, $[Na]_i$ are the intracellular concentrations of potassium, calcium and sodium respectively, F is Faraday's constant, ρ is the volume/surface area of the cell, and f is the ratio of free to total intracellular calcium. The extracellular bulk concentrations are assumed to change negligibly.

The form used for the pump transmission coefficient is:

$$\kappa_{pump} = a + \sqrt{u_1^2 + u_2^2}\,\frac{\tanh(b\theta)}{c} \times \frac{\tanh(d(\theta - e)) + 1}{2} \tag{65}$$

where $\theta = \arctan(u_1/u_2)$; u_1 and u_2 are the clock variables determined by the following differential equations:

$$\frac{du_1}{dt} = \omega\left[u_2 + u_1\left(1 - u_1^2 - u_2^2\right)\right] \tag{66}$$

$$\frac{du_2}{dt} = \omega\left[-u_1 + u_2\left(1 - u_1^2 - u_2^2\right)\right], \tag{67}$$

where ω is the intrinsic frequency of the waveform. At this stage, u_1 and u_2 have not been identified with physiological components in the model, but are assumed to be related to oscillat-

Table 1

The parameter values used in the model

Parameter	Units	Value
$[Na]_{i,initial}$	mM	19.0
$[Ca]_{i,initial}$	mM	2.0×10^{-4}
$[K]_{i,initial}$	mM	100.0
$[Na]_e$	mM	137.0
$[Ca]_c$	mM	2.5
$[K]_e$	mM	6.0
[ATP]	mM	4.99
[ADP]	mM	4.95
$[P_i]$	mM	0.06
T	K	310.15
τ	cm	10^{-6}
ρ	cm	1.5×10^{-4}
ω	counts/min	4.0
C_m	F/cm^2	2.0×10^{-6}
$K_{NaK,p}$	mol/cm^2 s	2.6×10^{-12}
$K_{Ca,p}$	mol/cm^2 s	8.0×10^{-13}
$K_{NaCa,e}$	mol/cm^2 s	4.0×10^{-11}
$(\mu^0_{ATP}-\mu^0_{ADP}-\mu^0_{P_i})/RT$	none	16.2
$(\mu^0_{Na_i}-\mu^0_{Na_e})/RT$	none	0.0
$(\mu^0_{Ca_i}-\mu^0_{Ca_e})/RT$	none	0.0
$(\mu^0_{K_i}-\mu^0_{K_e})/RT$	none	0.0
(κ_{pump}): a, b, c, d, e	none	0.05, 7.0, 7.0, −0.6, 2.0
f	none	0.0002

ing components such as cyclic nucleotides. Parameters a, b, c, d, e determine the shape of the transmission coefficient: a represents the basal value of the transmission coefficient or the normalized concentration of metabolic components during rest, b and d influence the upstroke and downstroke of the transmission coefficient respectively, while c and e mainly affect the magnitude and width of the transmission coefficient, although b and d also play a role.

The parameter values used are shown in Table 1 (parameters for the channels are not shown). [ATP], [ADP], $[P_i]$ are taken from Chapman et al. [5], and sodium, potassium and calcium concentrations are taken from Casteels [16]. Using a sodium–potassium reversal potential of -200 mV and a free energy of ATP splitting of $-19RT$, both approximated from DeWeer [44] and Chapman [45], $(\mu^0_{ATP}-\mu^0_{ADP}-\mu^0_{P_i})$ is $16.2RT$. Lucchesi et al. [14] have shown that the low levels of cytosolic calcium that exist in resting smooth muscle could be maintained solely by the operation of the plasmalemmal calcium pump. They obtained a transmembrane flux of 3.47×10^{-13} mol/cm^2 s for the ATP-dependent calcium transport. Using similar conditions in our expression for the calcium pump, a value of about $K_{Ca,p}=8\times10^{-13}$ mol/cm^2 s is obtained. Casteels [16] obtained 22.2 pmol/cm^2 s of sodium efflux via the sodium–potassium pump and Baker [37] obtained values of 10–20 pmol/cm^2 s of calcium efflux via the sodium–calcium exchanger. Using $K_{NaK,p}=2.6\times10^{-12}$ and $K_{NaCa,e}=4.0\times10^{-11}$ mol/cm^2 s in the model gives basal values of 42 pmol/cm^3 s of sodium efflux via the sodium–potassium pump and 13 pmol/cm^2 s of calcium efflux via the sodium–calcium exchanger. There are many changing parameters (for example, the ionic and metabolic concentrations and voltage) so that a strict comparison is not possible. However, the chosen values of $K_{Ca,p}$, $K_{NaK,p}$ and $K_{NaCa,e}$ are in agreement with the fact that carrier rates are known to be faster than pump rates [46]. In the absence of specific experimental data, it is assumed that there are no solubility differences between the intracellular and extracellular concentrations, i.e., $\mu^0_{I_i}-\mu^0_{I_c}=0$ for $I=$ Na, Ca, K. The parameters of the pump transmission coefficient (eq. 65) are not specifically obtained from experimental data, since variations of metabolic components in smooth muscle have not been determined quantitatively. In general, current–voltage experimental data is not available for active transport mechanisms in smooth muscle due to difficulties with the experimental preparation and the lack of specific inhibitors.

5. Simulation results

The differential equations of the model, eqs. (60), (62), (63), (64), (66), and (67) are simultaneously solved in a dimensionless form by using LSODE, a double precision subroutine capable of handling stiff systems of first order ordinary differential equations which is based on the Gear method [47]. The underlying processes can be described as follows: The electrical activity is

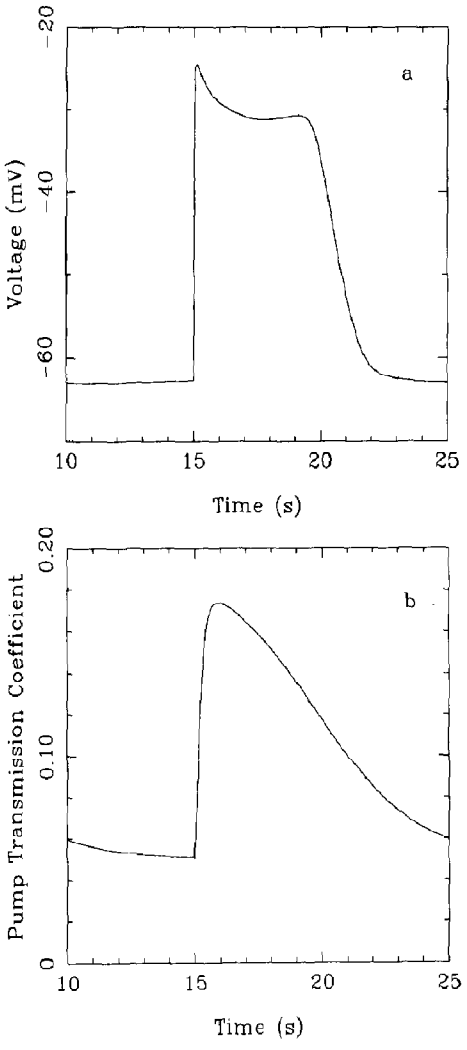

Fig. 1. (a) The voltage waveform of gastric smooth muscle, and (b) the pump transmission coefficient used.

initiated by a metabolic or subcellular clock which is reflected through the pump and channel transmission coefficients. Calcium and sodium ions move into the cell via their respective channels causing the cell to depolarize. Potassium also starts to move out via voltage and calcium gated channels. Due to its slower kinetics, the cell does

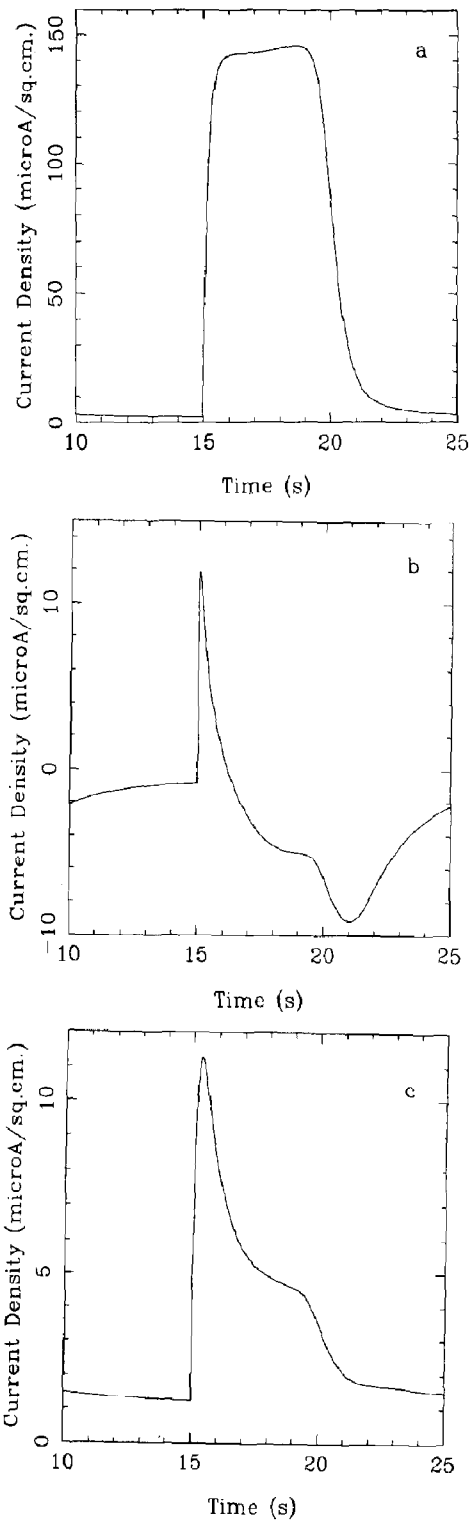

Fig. 2. (a) The calcium pump current density, (b) the sodium–calcium exchanger current density, and (c) the sodium–potassium pump current density.

not repolarize, but creates a rapid upshoot followed by a plateau region. The calcium channel kinetics change and the channels start to close, allowing the potassium ions to dominate and repolarize the cell. The movement of the ions are also affected by pumps and exchangers which work to maintain the ionic gradients in the cell.

The waveform obtained is shown in Fig. 1a and the pump transmission coefficient used is given in Fig. 1b. The current densities for the calcium pump, the sodium–calcium exchanger and the sodium–potassium pump are shown in Fig. 2a–c, respectively. The positive and negative current densities for the sodium–calcium exchanger illustrate its ability to change modes and move calcium and sodium both in and out. The voltage waveform compares well with that observed in gastric smooth muscle (human antrum) [48] with a plateau amplitude of about 30 mV and a resting membrane voltage of about −65 mV and an upshoot of about 5 mV.

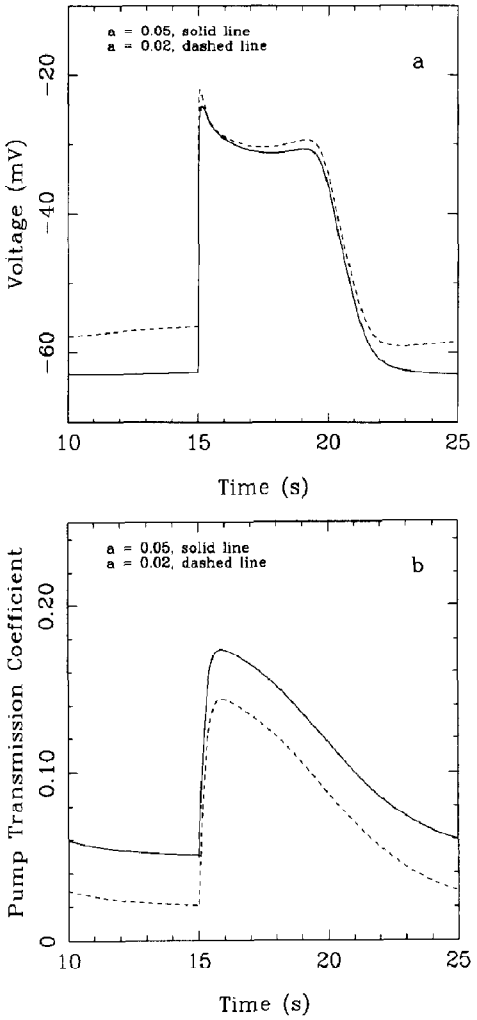

Fig. 3. (a) The voltage waveform with the *a* pump transmission coefficient parameter (or basal value) decreased from 0.05 to 0.02, (b) the pump transmission coefficient with its *a* value decreased from 0.05 to 0.02.

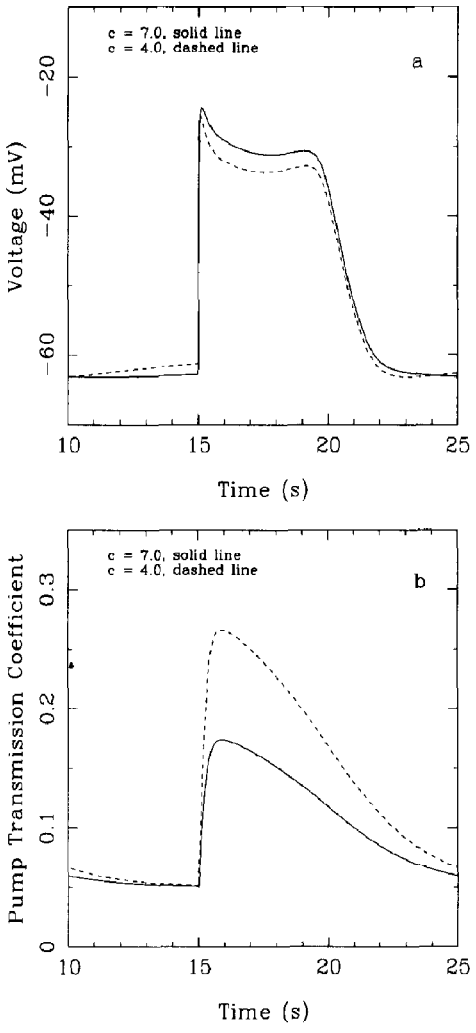

Fig. 4. (a) The voltage waveform with the *c* pump transmission coefficient parameter decreased from 7.0 to 4.0, and (b) the pump transmission coefficient with its *c* value decreased from 7.0 to 4.0.

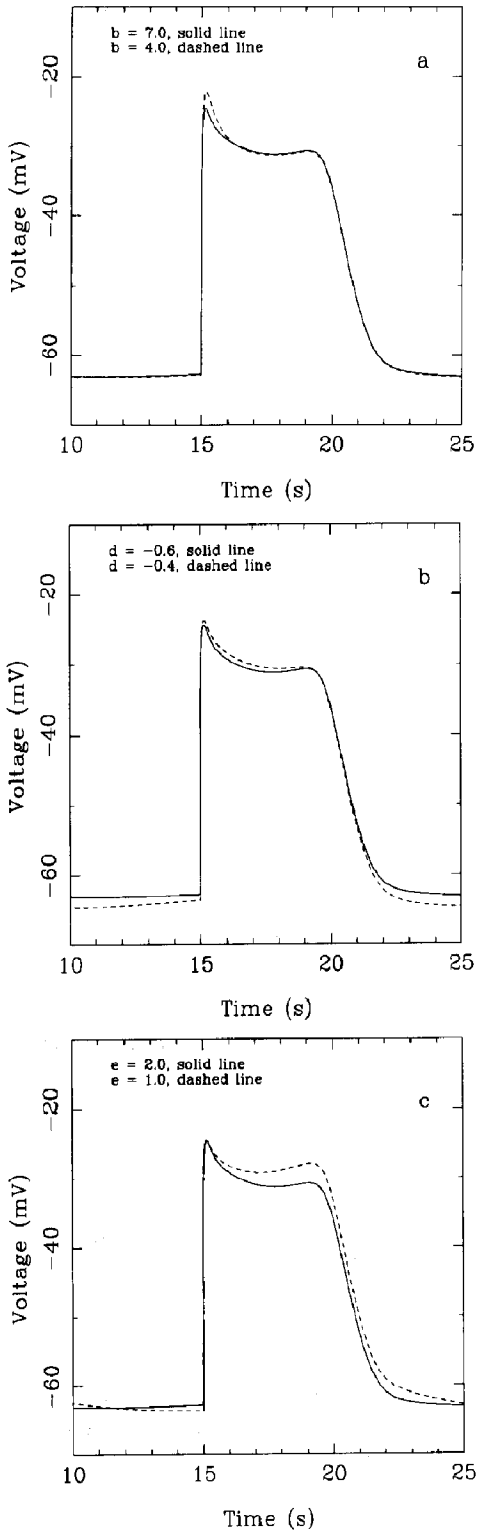

To illustrate the effect of the pumps and exchangers in the model, parameter changes are made in: (i) the pump transmission coefficient, κ_{pump}, (ii) the equilibrium exchange rates, $K_{Ca,p}$, $K_{NaK,p}$, $K_{NaCa,c}$ and (iii) [ATP] and the energy released from ATP splitting.

When the parameters in the pump transmission coefficient, eq. (65), are changed, we find the following: The basal value, a, affects the amplitude, b affects the upshoot, c affects the upshoot, amplitude and resting voltage, d affects the resting voltage and amplitude and e affects the plateau and resting voltage (Fig. 3–5).

Figure 3a illustrates the effect on the membrane voltage when the basal value, a, is reduced from 0.05 to 0.02. The pump transmission coefficient is shown in Fig. 3b for the same changes in the basal value, a. As may be seen in Fig. 3a, there is a decrease in the amplitude accompanied by a depolarizing change in the resting level, as a result of the change shown in Fig. 3b.

In the stomach, there is an observed amplitude variation [23]: In the forad direction, the amplitude decreases and the resting voltage depolarizes. These two observations are shown in the model: As the value of a decreases, the amplitude decreases and the resting voltage depolarizes. This suggests that the effects are not independent and that the observed gradient is due to different resting levels of metabolic components.

Figure 4a illustrates the effect on the membrane voltage when c (of eq. 65) is decreased from 7.0 to 4.0. Figure 4b shows the pump transmission coefficient for the c parameter change. Changing the c value can cause a prepotential in the membrane voltage, as shown in Fig. 4a.

Cells whose voltage oscillations are generated by membrane events show prepotentials in the waveform as the threshold for action potential generation is approached. As shown here, when a

Fig. 5. (a) The voltage waveform with the b pump transmission coefficient parameter decreased from 7.0 to 4.0, (b) The voltage waveform with the d pump transmission coefficient parameter increased from −0.6 to −0.4, and (c) the voltage waveform with the e pump transmission coefficient parameter increased from 2.0 to 1.0.

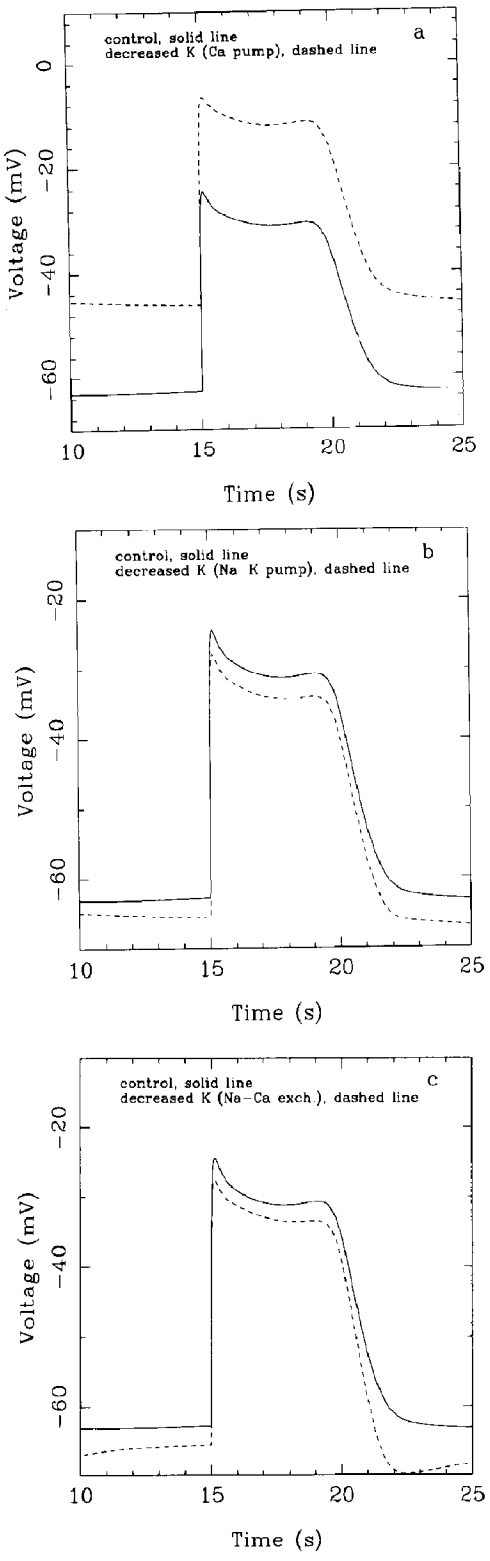

prepotential is present in the voltage waveform, the oscillations are not necessarily generated by membrane events, but could be due to metabolic or subcellular events.

The effect of changing the equilibrium exchange rates of the pumps and exchanger is shown in Figs. 6a–c. The calcium pump exchange rate, $K_{Ca,p}$, is decreased from 8.0×10^{-13} to 8.0×10^{-14} mol/cm^2 s in Fig. 6a, the sodium–potassium pump exchange rate, $K_{NaK,p}$, is decreased from 2.6×10^{-12} to 2.6×10^{-13} mol/cm^2 s in Fig. 6b, and the sodium–calcium exchanger exchange rate, $K_{NaCa,e}$, is decreased from 4.0×10^{-11} to 4.0×10^{-12} mol/cm^2 s in Fig. 6c. Decreasing $K_{Ca,p}$ depolarizes the waveform, since less calcium is being extruded. Decreasing $K_{NaCa,e}$ causes an after-hyperpolarization in the waveform. Decreasing $K_{NaK,p}$ hyperpolarizes the waveform.

Since the sodium–potassium pump has a net outward current, one might expect a decrease in $K_{NaK,p}$ to decrease the outward current and cause a depolarization in the waveform. However, there is a hyperpolarization in the waveform. Decreasing $K_{NaK,p}$ does decrease its outward current density. Due to the smaller sodium–potassium pump current density, the sodium–calcium exchanger current density decreases since less sodium is being removed by the pump so that less needs to be brought in by the exchanger. However, as less sodium is brought in by the exchanger, less calcium is removed by the exchanger so that the calcium pump current density increases to extrude the calcium. The increased outward calcium pump current density causes a hyperpolarization in the membrane voltage. This nicely illustrates the importance of the interactions between the various mechanisms. If the calcium pump and the sodium–calcium ex-

Fig. 6. (a) The voltage waveform with the equilibrium exchange rate of the calcium pump decreased from 8.0×10^{-13} to 8.0×10^{-14} mol/cm^2 s. (b) The voltage waveform with the equilibrium exchange rate of the sodium–potassium pump decreased from 2.6×10^{-12} to 2.6×10^{-13} mol/cm^2 s. (c) The voltage waveform with the equilibrium exchange rate of the sodium–calcium exchanger decreased from 4.0×10^{-11} to 4.0×10^{-12} mol/cm^2 s.

changer were not present in the model, decreasing $K_{NaK,p}$ would necessarily depolarize the membrane voltage.

With the pump and exchanger expressions, exchange rate changes in one mechanism affects the others. For example, decreasing $K_{Ca,p}$ necessarily decreases the calcium pump current density, but it also increases the sodium–calcium exchanger current density, that is, since the calcium pump is not as 'strong', the exchanger must work harder to extrude calcium. In turn, this causes more sodium to move into the cell so that the sodium–potassium pump must work harder to remove the sodium.

Increasing the ATP concentration or the amount of energy released from ATP splitting hyperpolarizes the membrane voltage. The effect on the membrane voltage when [ATP] is increased from 4.99 to 7.425 mM is shown in Fig. 7a. When the energy released from ATP splitting is increased from 16.2RT to 17.2RT, the effect on the membrane voltage is shown in Fig. 7b. A higher concentration of ATP provides more energy for the pumps as does an increase in the energy released from ATP splitting. Since both pumps have an outward current density, more energy increases this current density and hyperpolarizes the membrane voltage. In the case where the energy released from ATP splitting is increased a prepotential is also apparent.

The importance of active transport mechanisms in sodium–calcium interactions has been recognized [49]. Blocking the sodium–potassium pump with ouabain can cause a membrane depolarization of 10–15 mV or a depolarization to the level of the slow wave amplitude [22,29,49,50]. In addition, a probable link between membrane hyperpolarization and the activation of a calcium pump in the plasma membrane has been found [51]. More recently, the inhibition of calcium extrusion (calcium pump and sodium–calcium exchanger) was found to significantly inhibit smooth muscle relaxation [52]. This suggests that without the calcium pump, the cell would remain in a depolarized state.

The effect of ouabain is not simulated by decreasing $K_{NaK,p}$, the equilibrium exchange rate of the sodium–potassium pump, alone. As shown in Fig. 6b, this leads to a hyperpolarization of the waveform. However, a depolarization is obtained if the concentration of ATP or the amount of energy released from ATP splitting is decreased (Fig. 7). This suggests that the large depolarization obtained with ouabain is due to its effect on ATP. In other words, ouabain blocks the sodium–potassium pump by its effect on ATP rather than on $K_{NaK,p}$, the equilibrium exchange rate. Blocking sodium channels with TTX does not significantly affect the waveform [22,48],

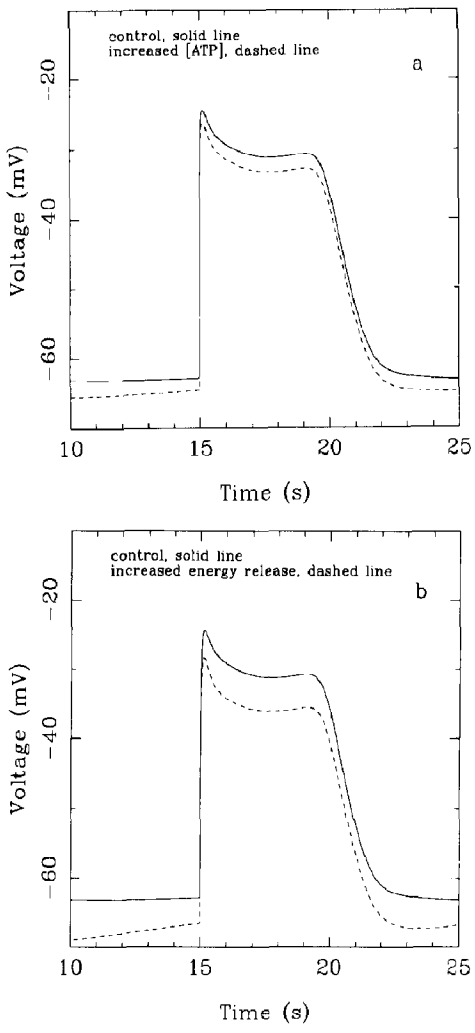

Fig. 7. (a) The voltage waveform with [ATP] increased from 4.99 mM to 7.425 mM, and (b) the voltage waveform with the energy released from ATP splitting increased from 16.2RT to 17.2RT.

whereas calcium channel blockers are known to suppress the plateau voltage [23,48]. This implies that sodium is not as major a player as calcium. Our simulations suggest that the large depolarization obtained with ouabain is due to its effect on ATP which not only affects the sodium–potassium pump but also the calcium pump which causes the depolarization. For this effect, the natural coupling that occurs between the active transport mechanisms is critical.

6. Discussion

In this paper we have presented a novel approach whereby thermodynamic representations for calcium pumps, sodium–potassium pumps and sodium–calcium exchangers have been included together in a model of ionic transport mechanisms for smooth muscle. Variations in basal metabolic concentrations were used to explain the two oppositely oriented gradients in the intrinsic magnitude of the membrane voltage and to show that these gradients are not independent. Coupling between pump and exchanger mechanisms is not hypothesized, but arises as a natural consequence of the electrochemical potential. This coupling has provided a possible explanation for the large depolarization obtained with ouabain: Ouabain blocks the sodium–potassium pump by its effect on ATP, which also affects the calcium pump. The sodium–calcium exchanger is known to exhibit several modes of operation [e.g. 37]. In our model of smooth muscle, the forward and reverse modes have arisen as a natural consequence of the interactions within the model.

Active transport mechanisms are needed in the cell membrane to maintain the asymmetric distribution of ionic concentrations. Without these mechanisms, the concentration gradients would run down and the cell would soon lose its ability to produce voltage oscillations. Experimentally, it is difficult to isolate and study pumps and exchangers and there is a lack of molecular information, e.g., the sodium–calcium exchanger protein has not yet been characterized and inhibitors have not yet been found [13]. A model offers a possible alternative to study these mechanisms. A model has the added advantage that it can dynamically consider all the mechanisms in the system. This is important since a pump or exchanger is not meant to function in an isolated environment. In smooth muscle, the added importance of metabolic components in the generation of oscillations increases the need to include these mechanisms in some detail, despite the lack of specific experimental data.

Most of the modelling approaches have focused on the sodium–potassium pump, since this is where most of the work has been done, and explicit reaction schemes have been developed. In performing a kinetic analysis of an explicit reaction scheme, it is necessary to know the forward and backward rates of each step. A steady-state situation is assumed in order to solve the system of equations (e.g. [5]). A net flux occurs by inclusion of voltage dependencies in one or more steps of the reaction cycle. The voltage dependence is usually assumed to take the form of a symmetric Eyring barrier (e.g. [4]). The assumptions that have been used by those performing kinetic analyses of explicit reaction schemes are: (i) steady state, (ii) the form of voltage dependence, and (iii) the step(s) in which voltage dependence occurs.

In our approach, nonequilibrium thermodynamics is used to develop expressions for the pump and exchanger current densities. SRT gives a functional form for the net rate of the reaction. This functional form is not empirically derived and does not rely on assumptions such as a linear dependence on how far the reaction is removed from equilibrium. Instead, SRT has its basis in quantum and statistical mechanics. In this approach, neither steady state nor the form and location of voltage dependence are assumed. The functional form of the voltage dependence is due to SRT (by its presence in the electrochemical potential) and there is no need to assume a symmetric Eyring barrier. The assumptions made are: (i) the presence of a rate-limiting step in the reaction scheme, and (ii) a ratio of intermediate substrates that does not vary significantly from its equilibrium ratio. Under these conditions, the explicit reaction scheme is not required to obtain the pump or exchanger current density expres-

sion. However, information on these reaction schemes is needed to determine whether the required assumptions are valid. This advantage has allowed us to obtain expressions not only for the sodium–potassium pump, but also the calcium pump and the sodium–calcium exchanger.

This thermodynamic approach assumes that there is a rate-limiting step in the reaction scheme. This is a strong assumption, but at present, there is insufficient evidence to exclude this possibility. In a detailed physical mechanism for the sodium pump, Levitt [53] took the approach that the enzyme cycled through only three kinetic states during the normal operation of the pump and that one of the transitions was rate-limiting. In the interpretation of steady state current–voltage relationships, DeWeer et al. [54] suggested that the overall voltage dependence of the cycle may reflect that of a rate-limiting step or that of the steady state level of the intermediate entering that step. The assumptions of a rate-limiting step in the reaction scheme is a first approximation, but with no further experimental data, there is no reason to use a more complicated form. It has allowed us to obtain a relatively simple functional form for the pump and exchanger current densities. However, this functional form is *independent* of the particular rate-limiting step. This implies that if different physiological conditions resulted in different rate-limiting steps, the functional form would not change, only the value of K, the equilibrium exchange rate. Also, with a lack of specific experimental data for smooth muscle, a simple functional form is helpful in reducing the number of parameters to be determined.

The new expressions for the calcium pump, sodium–potassium pump and sodium–calcium exchanger were included with the passive transport mechanisms and the effect of each active transport mechanism as well as their interactions was examined. Decreased equilibrium exchange rates of the calcium pump, or increased equilibrium exchange rates of the sodium–potassium pump and the sodium–calcium exchanger depolarized the membrane voltage. Decreasing any of the equilibrium exchange rates affected the current densities of all the active mechanisms since there are interactions via voltage, intracellular and extracellular concentrations, metabolic concentrations and the amount of energy released from ATP splitting. Increasing the concentration of ATP or the amount of energy released from ATP splitting led to a hyperpolarization of the waveform. The importance of the pump transmission coefficient in this approach should be recognized. The oscillations in smooth muscle have been shown to be generated by metabolic, and not voltage dependent processes [17]. Therefore, it was introduced in this model of smooth muscle to represent the oscillatory and normalized time-variation of metabolic components. The specific form of the pump transmission coefficient was chosen to give the most realistic voltage waveform. Its particular parameters affected the amplitude, resting and plateau voltage of the waveform.

The experimental data required for this approach not only involves knowledge of whether a rate-limiting step is present in the reaction scheme, and the equilibrium exchange rate for the rate-limiting step, but also how the metabolic components are expected to vary. This knowledge, together with current–voltage data will allow this approach to be evaluated. The behaviour of the metabolic components is especially important, since it will determine the form of the pump transmission coefficient. At present, such data is not available for smooth muscle. Instead, an overall model was developed and the parameters for the pump transmission coefficient were chosen to balance the concentrations in the model during the known physiological behaviour of the membrane voltage waveform in gastric smooth muscle. Given the importance of pumps in smooth muscle, expressions which were more than just linear dependencies on concentrations and which involved the cell's energy source were required. As it turned out, the approach adopted offers an alternative to modelling pumps and exchangers in a whole cell model.

Appendix A

The expressions for the channel current densities are given by a generalized form of the GHK

current equation. In this generalization, the assumption of local equilibrium and equal partition coefficients at the intracellular and extracellular bulk/channel interfaces is removed using SRT. They have the following form [21]:

$$J_I = \frac{D_I z_I^2 F^2 V_m}{\tau RT} \left\{ \frac{[C_I]_\tau - [C_I]_0 \exp\left(\frac{z_I F V_m}{RT}\right)}{1 - \exp\left(\frac{z_I F V_m}{RT}\right)} \right\} \tag{68}$$

and the channel/interfacial concentrations are determined from the following equations:

$$-\kappa_I K^i_{CB,I} \left\{ \frac{[C_I]_0}{\beta^i_I [I]_i} - \frac{\beta^i_I [I]_i}{[C_I]_0} \right\} = \kappa_I K^e_{CB,I} \left\{ \frac{[C_I]_\tau}{\beta^e_I [I]_e} - \frac{\beta^e_I [I]_e}{[C_I]_\tau} \right\} = \frac{z_I D_I F V_m}{\tau RT} \left\{ \frac{[C_I]_\tau - [C_I]_0 \exp\left(\frac{z_I F V_m}{RT}\right)}{1 - \exp\left(\frac{z_I F V_m}{RT}\right)} \right\} \tag{69}$$

(70)

where I is the particular ionic species, J is the current density, D is the diffusion coefficient, z is the valency, $[C_I]_0$, $[C_I]_\tau$ are the channel concentrations on the intracellular and extracellular sides of the membrane respectively, K^i_{CB}, K^e_{CB} are the equilibrium exchange rates across the channel interfaces on the intracellular and extracellular sides respectively, β^i, β^e are the intracellular and extracellular partition coefficients respectively and κ is the channel transmission coefficient which represents the gating.

Acknowledgements

This work was supported by the Medical Research Council of Canada and the Natural Science and Engineering Research Council of Canada.

References

1 C.A. Ward, R.D. Findlay and M. Rizk, J. Chem. Phys. 76 (1982) 5599.
2 R.A. Sjodin, in: Electrogenic transport: fundamental principles and physiological implications, eds. M.P. Blaustein and M. Lieberman (Raven Press, New York, 1984) p. 105.
3 R.C. Thomas, Physiol. Rev. 52 (1972) 563.
4 U.-P. Hansen, D. Gradmann, D. Sanders and C.L. Slaymann, J. Membr. Biol. 63 (1981) 165.
5 J.B. Chapman, E.A. Johnson and J.M. Kootsey, J. Membr. Biol. 74 (1983) 139.
6 J.B. Chapman, J.M. Kootsey and E.A. Johnson, J. Theor. Biol. 80 (1979) 405.
7 S.I. Rapoport, Biophys. J. 10 (1970) 246.
8 D.R. Lemieux, F.A. Roberge and P. Savard, J. Theor. Biol. 142 (1990) 1.
9 Y.S. Lee, T.R. Chay and T. Ree, Biophys. Chem. 18 (1983) 25.
10 F.K. Skinner and B.L. Bardakjian, J. Gastrointest Mot. 3 (1991) 213.
11 D.R. Lemieux, F.A. Roberge and D. Joly, J. Theor. Biol. 154 (1992) 335.
12 D. DiFrancesco and D. Noble, Phil. Trans. R. Soc. (London) B307 (1985) 353.
13 H.J. Schatzmann, in: Calcium and cell physiology, ed. D. Marmé (Springer-Verlag, New York, 1985) p. 18.
14 P.A. Lucchesi, R.A. Cooney, C. Mangsen-Baker, T.W. Honeyman and C.R. Scheid, Am. J. Physiol. 255 (1988) C226.
15 Y. Sakai, A. Isobe and S. Ichikawa, J. Membr. Biol. 89 (1986) 65.
16 R. Casteels, in: Smooth muscle: an assessment of current knowledge, eds. E. Bülbring, A.F. Brading, A.W. Jones and T. Tomita (Edward Arnold, London, 1981) Ch. 5.
17 J.D. Huizinga, L. Farraway and A. Den Hertog, J. Physiol. 442 (1991) 31.
18 C.A. Ward, J. Chem. Phys. 79 (1983) 5605.
19 C.A. Ward, J. Chem. Phys. 67 (1977) 229.
20 C.A. Ward and M. Elmoselhi, Surface Sci. 176 (1986) 457.
21 F.K. Skinner, Ionic transport mechanisms in a model of gastric smooth muscle, Ph.D. Thesis, University of Toronto (1992).
22 T. Tomita, in: Smooth muscle, an assessment of current knowledge, eds. E. Bülbring, A.F. Brading, A.W. Jones and T. Tomita, (Edward Arnold, London, 1981) Ch. 6.
23 J.H. Szurszewski, in: Physiology of the gastrointestinal tract, ed. L.R. Johnson (Raven Press, NY, 1987) p. 383.
24 P.E. Rapp and M.J. Berridge, J. Theor. Biol. 66 (1977) 497.
25 J.A. Connor, J. Exp. Biol. 81 (1979) 153.
26 M. Ohba, Y. Sakamoto and T. Tomita, J. Physiol. 253 (1975) 505.
27 D.D. Job, Am. J. Physiol. 220 (1971) 299.
28 M.J. Berridge and P.E. Rapp, J. Exp. Biol. 81 (1979) 217.
29 C.L. Prosser and A.W. Mangel, in: Cellular Pacemakers, ed. D.O. Carpenter (Wiley, New York, 1982) Ch. 10.

30 B.L. Bardakjian, S.D. Bot and M.M. Lau, Digest, Dis. Sci. 32 (1987) 902.
31 J. Keizer and G. Magnus, Biophys. J. 56 (1989) 229.
32 C.A. Ward, M. Rizk and A.S. Tucker, J. Chem. Phys. 76 (1982) 5606.
33 A.K. Grover, Cell Calcium 6 (1985) 227.
34 F. Wuytack, L. Raeymaekers and R. Casteels, Experientia 41 (1985) 900.
35 E. Carafoli and M. Zurini, Biochim. Biophys. Acta 683 (1982) 279.
36 E. Carafoli, Adv. Cycl. Nucl. Prot. Phosp. Res. 17 (1984) 543.
37 P.F. Baker, Ciba Foundation Symp. 122, 1986, p. 73.
38 M.P. Blaustein, Curr. Top. Membr. Transp. 34 (1989) 289.
39 E.E. Daniel, Experientia 41 (1985) 905.
40 C.C. Aickin, A.F. Brading and D. Walmsley, J. Physiol. 391 (1987) 325.
41 W.D. Stein, Channels, Carriers and Pumps: an introduction to membrane transport (Academic Press, 1990) Ch. 5.
42 E.A. Johnson and J.M. Kootsey, J. Membr. Biol. 86 (1985) 167.
43 P. Läuger and H.-J. Apell, Eur. Biophys. J. 13 (1986) 309.
44 P. DeWeer, in: Electrogenic transport: fundamental principles and physiological implications, eds. M.P. Blaustein and M. Lieberman (Raven Press, New York, 1984) p. 1.
45 J.B. Chapman, in: Electrogenic transport: fundamental principles and physiological implications, eds. M.P. Blaustein, M. Lieberman (Raven Press, New York, 1984) p. 17.
46 G. Sachs and S. Fleischer, Meth. Enzymol. 171 (1989) 3.
47 C.W. Gear, Numerical initial value problems in ordinary differential equations (Prentice-Hall, Englewood Cliffs, 1971).
48 T.Y. El-Sharkawy, K.G. Morgan and J.H. Szurszewski, J. Physiol. 279 (1978) 291.
49 C. van Breeman, P. Aaronson and R. Loutzenhiser, Pharmacol. Rev. 30 (1979) 167.
50 J.A. Connor, in: Electrogenic transport: fundamental principles and physiological implications, eds. M.P. Blaustein, M. Lieberman (Raven Press, New York, 1984) p. 271.
51 T. Tomita, A. Takai and H. Tokuno, Experientia 41 (1985) 963.
52 R.F. Willenbucher, Y. Xie, V.E. Eysselsin and W.J. Snape Jr., Gastroenterology 99 (1990), Abstract 115.
53 D.G. Levitt, Biochim. Biophys. Acta 604 (1980) 321.
54 P. DeWeer, D.C. Gadsby and R.F. Rakowski, Annu. Rev. Physiol. 50 (1988) 225.